Structure of [M + H −H 2 O] + from Protonated Tetraglycine Revealed by Tandem Mass Spectrometry and IRMPD Spectroscopy

ARTICLE *in* THE JOURNAL OF PHYSICAL CHEMISTRY C · JANUARY 2010

Impact Factor: 4.77

CITATIONS
3

READS
8

8 AUTHORS, INCLUDING:

Benjamin J. Bythell
University of Missouri - St. Louis
36 PUBLICATIONS **241** CITATIONS
SEE PROFILE

Jeffrey D. Steill
Oak Ridge National Laboratory
84 PUBLICATIONS **1,490** CITATIONS
SEE PROFILE

Gary S Groenewold
142 PUBLICATIONS **2,173** CITATIONS
SEE PROFILE

Michael J Van Stipdonk
Duquesne University
143 PUBLICATIONS **2,834** CITATIONS
SEE PROFILE

Structure of $[M + H - H_2O]^+$ from Protonated Tetraglycine Revealed by Tandem Mass Spectrometry and IRMPD Spectroscopy

Benjamin J. Bythell,[†] Ryan P. Dain,[‡] Stephanie S. Curtice,[‡] Jos Oomens,[§] Jeffrey D. Steill,[§] Gary S. Groenewold,[||] Béla Paizs,[†] and Michael J. Van Stipdonk[‡,*]

Computational Proteomics Group, German Cancer Research Center, Heidelberg, Germany, Department of Chemistry, Wichita State University, Wichita Kansas 67260-0051, FOM Institute for Plasma Physics "Rijnhuizen", Nieuwegein, The Netherlands, and Interfacial Chemistry Group, Idaho National Laboratory, Idaho Falls ID

Received: November 28, 2009; Revised Manuscript Received: February 7, 2010

Multiple-stage tandem mass spectrometry and collision-induced dissociation were used to investigate loss of H_2O or CH_3OH from protonated versions of GGGX (where X = G, A, and V), GGGGG, and the methyl esters of these peptides. In addition, wavelength-selective infrared multiple photon dissociation was used to characterize the $[M + H - H_2O]^+$ product derived from protonated GGGG and the major MS^3 fragment, $[M + H - H_2O - 29]^+$ of this peak. Consistent with the earlier work [Ballard, K. D.; Gaskell, S. J. *J. Am. Soc. Mass Spectrom.* **1993**, *4*, 477−481; Reid, G. E.; Simpson, R. J.; O'Hair, R. A. J. *Int. J. Mass Spectrom.* **1999**, *190/191*, 209−230000], CID experiments show that $[M + H - H_2O]^+$ is the dominant peak generated from both protonated GGGG and protonated GGGG−OMe. This strongly suggests that the loss of the H_2O molecule occurs from a position other than the C-terminal free acid and that the product does not correspond to formation of the b_4 ion. Subsequent CID of $[M + H - H_2O]^+$ supports this proposal by resulting in a major product that is 29 mass units less than the precursor ion. This is consistent with loss of $HN{=}CH_2$ rather than loss of carbon monoxide (28 mass units), which is characteristic of oxazolone-type b_n ions. Comparison between experimental and theoretical infrared spectra for a group of possible structures confirms that the $[M + H - H_2O]^+$ peak is not a substituted oxazolone but instead suggests formation of an ion that features a five-membered ring along the peptide backbone, close to the amino terminus. Additionally, transition structure calculations and comparison of theoretical and experimental spectra of the $[M + H - H_2O - 29]^+$ peak also support this proposal.

Introduction

Low-energy collision-induced dissociation (CID) of protonated peptides enables proton transfer(s) to occur prior to intramolecular nucleophilic attack, leading to cleavage of amide bonds and formation of b, y, and a ions.[1] The mobilization of protons to enable amide bond cleavage[2] is described by the "mobile-proton" model of peptide fragmentation.[2f] Spectroscopic[3] and hydrogen/deuterium exchange[4] data have provided direct evidence for this model and for the mobility of protons in protonated peptides in mass spectrometers.

Formation of b and/or y sequence ions occurs on the b_n-y_m pathway(s)[5] in complementary reactions. It is generally accepted that the C-terminal y_m fragments generated in these reactions are truncated peptides.[6] Recently, the structure and reactivity of the complementary N-terminal b_n ions have received a large amount of attention. While these ions were originally thought to be truncated peptides with a C-terminal, charged acylium group ($-C{\equiv}O^+$),[1b] it is now believed that most small b_n ions ($n \leq 4$) are terminated by the five-membered oxazolone ring at the C-terminus.[7] Experimental evidence supporting the oxazolone structure for small b_n ions was provided by CID studies,[7,8] gas-phase "action" infrared spectroscopy,[3,9] H/D exchange,[6b,10] and neutralization−reionization MS[11] work on various b ions. The oxazolone structure is also supported by numerous computational studies.[8d,9,11,12] On the other hand some b_2 ions from some histidine containing peptides have been shown to have a mixture of protonated oxazolone and diketopiperazine structures.[13] A wealth of recent evidence also points to larger b_n ions ($n \geq 5$) primarily adopting O-protonated, macrocyclic peptide structures.[14]

Here, tandem mass spectrometry and infrared multiple photon dissociation (IRMPD) were used to investigate the nominally "b_4 ion" generated by dehydration of a series of model peptides. This type of ion is widely assumed to result from a conventional b_n-y_m[15] oxazolone-forming reaction, which involves bond cleavage at the C-terminus (eliminating H_2O in this case) and an additional proton (illustrated in Scheme 1a for singly protonated tetraglycine). For protonated tetraglycine this reaction would result in a b_4 ion with a C-terminal oxazolone ring. The most favorable sites of protonation of this b_4 ion are the oxazolone ring nitrogen, or the N-terminus (Figure 1, structures **I** and **II** respectively). The possible adoption of at least one alternative, nonresidue specific water loss structure was first suggested by Ballard and Gaskell[16] but no structure was postulated to explain their findings. Later, Reid et al.[6b] proposed a retro-Ritter-like reaction (Scheme 1b) involving "backbone−backbone neighboring group participation reactions" as a means of eliminating water. Such a pathway involves elimination of an amide carbonyl O atom along with 2 H atoms

* Corresponding author. E-mail: mike.vanstipdonk@wichita.edu.
[†] German Cancer Research Center.
[‡] Wichita State University.
[§] FOM Institute for Plasma Physics "Rijnhuizen".
[||] Idaho National Laboratory.

10.1021/jp9113046
Published on Web 03/30/2010

SCHEME 1: Loss of H_2O from Protonated GGGG: (a) Conventional b_n-y_m[15] Oxazolone-Forming Pathway, (b) "Retro-Ritter Type" Process[6b] with Elimination of an Amide O Atom

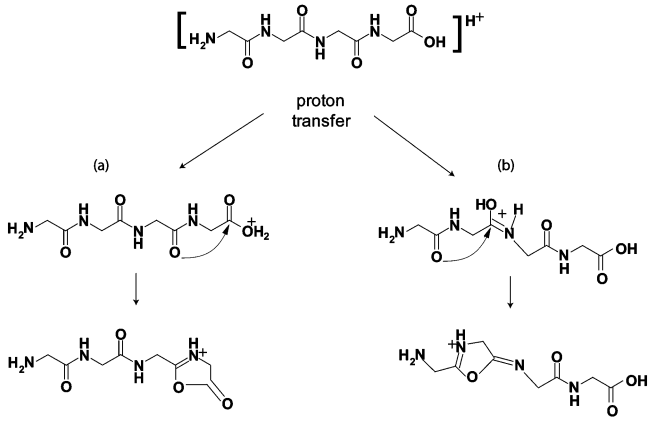

and can conceivably occur anywhere along the backbone other than the C-terminus. Conversely, such reactions were shown not to be active from shorter aliphatic peptides.[17] Structures **III**−**VIII** in Figure 2 illustrate some possible species resulting from these two types of reaction pathway for protonated tetraglycine. Here we investigate these two general classes of potential product ion. The significant structural differences and protonation arrangements between these two classes of potential product ion make these systems excellent candidates for identification by means of infrared "action" spectroscopy (coupled to tandem mass spectrometry). The goal of the current study was to determine which of these structures corresponds to the $[GGGG + H - H_2O]^+$ ion generated in the mass spectrometer.

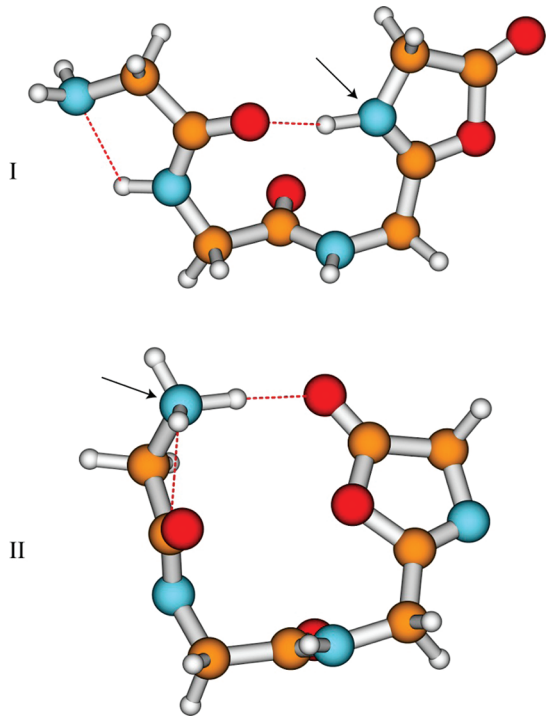

Figure 1. Lowest energy b_4 structures determined at the B3LYP/6-31+G(d,p) level of theory with the relative energies corrected for zero-point vibration energy (ZPE) at the B3LYP/6-31G(d): structure **I**, oxazolone nitrogen protonated; structure **II**, oxazolone N-terminally protonated. The site of protonation in each case is indicated with an arrow.

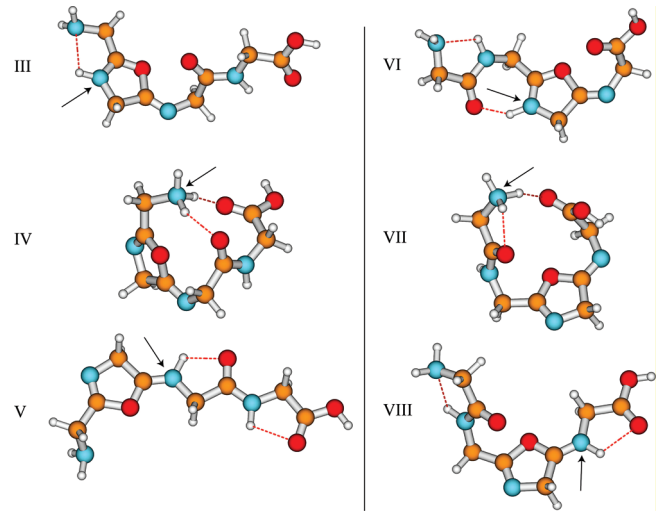

Figure 2. Various possible H_2O loss ions determined at the B3LYP/6-31+G(d,p) level of theory with the relative energies corrected for zero-point vibration energy (ZPE) at the B3LYP/6-31G(d): structure **III**, ring protonated; structure **IV**, N-terminally protonated; structure **V**, imine protonated; structure **VI**, protonated five-membered ring in the middle of the peptide backbone; structure **VII**, N-terminally protonated structure, with five-membered ring in the middle of the peptide backbone; structure **VIII**, imine protonated structure, with five-membered ring in the middle of the peptide backbone. The site of protonation in each case is indicated with an arrow.

Experimental and Computational Section

Peptide Synthesis. GGGG and GGGGG were purchased from Fisher Scientific and used as received. GGGA, GGGV, and AGGG were synthesized by solid-phase methods using FMOC-protected amino acids and conventional coupling procedures. All peptides were used without further purification. Methyl esters of the respective peptides were generated by incubation in CH_3OH with trace HNO_3 for 8 h, followed by complete evaporation of solvent.

Quadrupole Ion Trap CID. Quadrupole ion trap CID of the protonated peptides was explored using a Finnigan LCQDeca ion trap mass spectrometer (Thermo Fisher Scientific, San Jose CA). Solutions of each peptide and peptide−methyl ester were prepared by dissolving the appropriate amount of solid material in a 1:1 (v:v) mixture of CH_3OH and H_2O or CH_3OD and D_2O to produce final concentrations of $\sim 10^{-4}$ to 10^{-3} M. A small amount of trifluoroacetic acid was added to enhance protonation. Peptide solutions were infused into the ESI instrument using the incorporated syringe pump at a flow rate of 5 μL/min. The atmospheric pressure ionization stack settings for the LCQ (lens voltages, quadrupole and octapole voltage offsets, etc.) were optimized for highest $[M + H]^+$ or $[M + D]^+$ ion intensity using the autotune routine within the LCQ Tune program. The spray needle voltage was maintained at +5 kV, N_2 sheath gas flow rate at approximately 0.375 L/min and the capillary (desolvation) temperature at 200 °C.

For CID studies, the precursor isolation widths used were 0.8−1.0 mass-to-charge (m/z) units to ensure the isolation and dissociation of a single isotopic peak in each case. The normalized collision energies (which define the amplitude of radiofrequency (rf) voltage applied to the end-cap electrodes to induced collisional activation) were set to 25−30% of 5 V, which corresponds to approximately 0.65−0.72 V in the laboratory frame of reference using the current instrument calibration. The activation Q setting (used to adjust the q parameter for the precursor ion during the CID experiment) was 0.30 and activation times of 30 ms were used.

IRMPD Spectroscopy. Infrared spectra were obtained by IRMPD spectroscopy using the Fourier transform ion cyclotron resonance (FTICR) mass spectrometer coupled to the beamline of the Free Electron Laser for Infrared eXperiments (FELIX) in The Netherlands, as described previously.[18] Briefly, ions are produced by electrospray ionization (ESI) and accumulated in a hexapole ion trap. The ions are then pulse injected into a home-built FTICR mass spectrometer,[19] where the ion of interest is isolated and then irradiated with FELIX for 2 s at a 5 Hz repetition rate. In these experiments, the wavelength of FELIX is tuned between ~5.26 and 7.8 μm and the pulse energy amounts to approximately 35 mJ per 5 μs pulse. After irradiation, parent and fragment ion intensities are recorded. Data acquisition and instrument control is accomplished using a modified version of the data system and software developed by Heeren and co-workers.[20]

ESI of the GGGG solution yielded an abundant $[GGGG + H]^+$ ion at *m/z* 247. When the rf amplitude and the axial trapping voltage of the accumulation hexapole are adjusted, conditions can be made such that the $[GGGG + H - H_2O]^+$ ion (*m/z* 229) and its fragmentation product at *m/z* 200, $[GGGG + H - 47]^+$, are formed by collision-induced dissociation in the ion source and transfer regions of the mass spectrometer. These ions can then be mass selected for irradiation with FELIX.

Upon resonant infrared irradiation with FELIX, the $[GGGG + H - H_2O]^+$ ion dissociates into an ion at *m/z* 200, consistent with observations following CID of the same ion (vide infra). An IRMPD spectrum of $[GGGG + H - H_2O]^+$ was generated from the precursor (I_{prec}) intensity and the sum of the fragment ion intensities (I_{frags}) after laser irradiation as a function of frequency:

$$\text{IRMPD yield} = \sum I_{frags}/(I_{prec} + \sum I_{frags})$$

The same approach was used to generate an IRMPD spectrum of $[GGGG + H - 47]^+$. Upon resonant irradiation, this precursor ion fragmented by elimination of 57 and 75 u. For both IRMPD spectra, the fragment yields were linearly corrected for variations in the laser pulse energy as a function of the energy of the incident photons.

Density Functional Theory Calculations

The potential energy surface (PES) of the various conceivable $[GGGG + H - H_2O]^+$ ions generated from protonated GGGG was investigated using the strategy developed recently to deal with protonated peptides and their fragments.[15a,c,21] These calculations began with molecular dynamics simulations using the Insight II program (Biosym Technologies, San Diego) in conjunction with a modified AMBER force field.[22] During the dynamics calculations simulated annealing techniques were used to produce candidate structures for further refinement, applying full geometry optimization using the AMBER force field. These optimized structures were analyzed by a conformer family search program that groups optimized structures into families for which the most important characteristic torsion angles are similar. The most stable species in the families were then fully optimized at the PM3, HF/3-21G, B3LYP/6-31G(d), and finally at the B3LYP/6-31+G(d,p) levels with the conformer families regenerated at each level. The Gaussian set of programs[23] was used for all ab initio and DFT calculations.

The relative energies of candidate structures were calculated by correcting the B3LYP/6-31+G(d,p) total energies for zero-point vibrational energy (ZPE) contributions determined from the unscaled B3LYP/6-31G(d) frequencies. Our prior studies[3,9,14a,c,e,24] have established that the predicted IR spectra determined at the B3LYP/6-311+G(d,p) level of theory provide good agreement with IRMPD spectra. Therefore, for structure determination, the IR spectra of the lowest-energy oxazolone and retro-Ritter-type products were determined following reoptimization at this level of theory. The resulting theoretical spectra were scaled by a factor of 0.98, which is commonly used in IRMPD studies of protonated peptides and peptide fragments in this frequency region.[3,9,15a,c,24e]

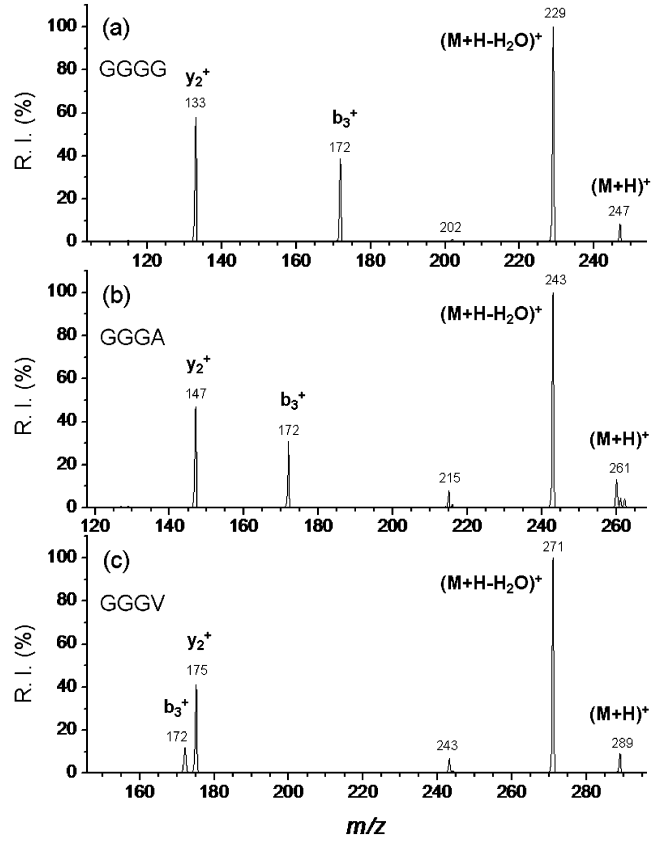

Figure 3. MS/MS spectra of protonated (a) GGGG, (b) GGGA, and (c) GGGV.

Results and Discussion

CID of GGGX and GGGX-OMe. Figure 3 shows CID spectra generated from protonated GGGG (a), GGGA (b), and GGGV (c). For each peptide, the dominant product ion is formed by loss of H_2O (*m/z* 229, 243, and 271, respectively). Due to the uncertainty regarding the actual structure of the species we refer to the ion from here on as $[M + H - H_2O]^+$. Also observed in the CID spectra are the b_3 (*m/z* 172 in each spectrum) and y_2 peaks (*m/z* 133, 147, and 175 for GGGG, GGGA, and GGGV, respectively). The observations made here with respect to the CID of protonated GGGG are entirely consistent with earlier work by Reid and co-workers,[6b] in which the fragmentation of protonated polyglycines was investigated using multiple-stage (MS^n) tandem mass spectrometry. Additionally, these[6b] and other authors[10,13,14f] have used hydrogen/deuterium exchange (HDX) to investigate the ion structures of b and other ions produced by CID of protonated peptides.

The dominant fragmentation pathway for oxazolone b_n ions is elimination of carbon monoxide (28 mass units (u)) to furnish the corresponding a_n ions.[1c,7,25] Conversely, the product ion spectra (MS^3 stage) of the $[M + H - H_2O]^+$ derived from

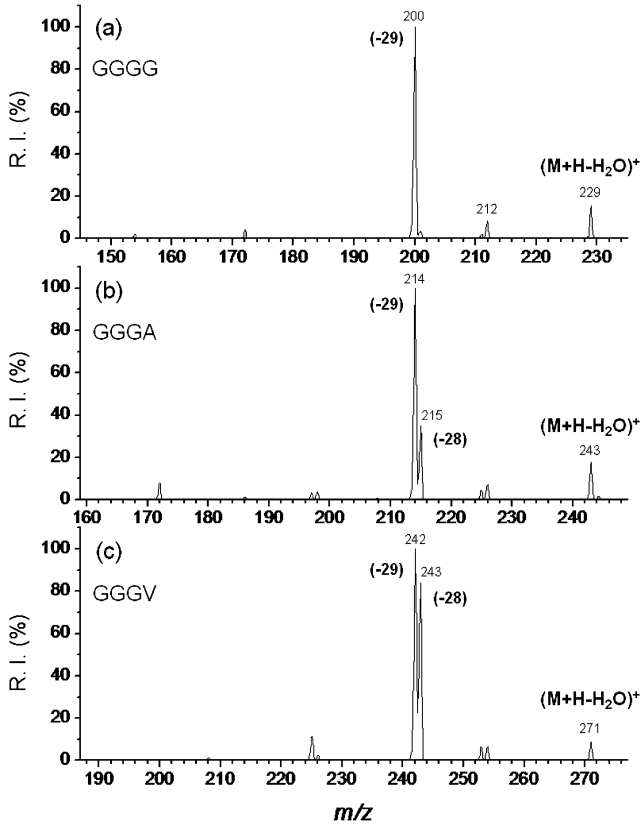

Figure 4. MS^3 spectra generated from the $[M + H - H_2O]^+$ ion derived from protonated (a) GGGG, (b) GGGA, and (c) GGGV.

protonated GGGG, GGGA, and GGGV (Figure 3) show the dominant product ion to be 29 u less than the precursor. This loss of 29 u shifts to a loss of 43 u for CID of $[AGGG + H - H_2O]^+$ from AGGG (spectrum not shown), indicating that the dissociation reaction involves elimination from the amino terminus of the $[M + H - H_2O]^+$ ion, consistent with elimination of $H_2C{=}NH$ and $H_3CHC{=}NH$, respectively. This finding clearly precludes alternative reaction pathways analogous to the "diketopiperazine" route to b_n ions, in which structures are generated that incorporate a six-membered ring into the N-terminus[6] (see Figures S4 and S5, Supporting Information, for further details). Additionally, the peak attributable to formation of a_4 ion (m/z 201) is only ca. 2% relative intensity (Figure 4a), indicating that the b_4 ion was only a minor component of the $[GGGG + H - H_2O]^+$ peak. The relative intensity of the corresponding a_4 ion is higher in the product ion spectra generated from dehydated GGGA and GGGV (Figure 4b,c, respectively), though elimination of 29 u remains a competitive pathway. This observation suggests that the formation of the oxazolone b_4 product is sensitive to the identity of the C-terminal amino acid. The a_4 product peaks in Figure 4a−c are diagnostic for the generation of the b_4 ion via loss of H_2O from the C-terminus of the peptides. The CID results for this set of peptides demonstrate that the b_4 ion makes up, at most ~50% of the total $[M + H - H_2O]^+$ ion population, and considerably less than this when the C-terminal residue is glycine.

Methyl esterification of the C-termini of the GGGX peptides (X = G, A, V) followed by tandem mass spectrometry leads to conclusions similar to the preceding findings for the normal peptides (Figure S1, Supporting Information), namely, that H_2O elimination can occur remote from the C-terminus of the peptide and thus likely involves elimination of an amide carbonyl O atom. Comparison of the spectra resulting from the $[M + H - CH_3OH]^+$ peaks derived from GGGG-OMe, GGGA-OMe, and GGGV-OMe (Figure S-2, Supporting Information) indicated that the dominant product ions generated occur at m/z 201, 215, and 243 for GGGG−OMe, GGGA−OMe, and GGGV−OMe, respectively, corresponding to elimination of 28 u (CO), consistent with fragmentation of a b_4 oxazlone structure. Conversely, the spectra resulting from the $[M + H - H_2O]^+$ ions (Figure S3, Supporting Information) show dominant loss of 29 u, consistent with the results shown in Figure 4 for dissociation of $[M + H - H_2O]^+$ derived from the free acid forms of the peptides. This MS^n data supports the hypothesis that b_4 ion is not a major product generated by CID of protonated GGGG and represents only a fraction of the $[M + H - H_2O]^+$ ion population created from GGGA and GGGV. Our results agree well with the earlier work by Reid and co-workers,[6b] in particular with the HDX experiments that demonstrated distinct exchange behavior for $[M + H - H_2O]^+$ created from protonated GGGG and b_4 generated by CID of protonated GGGGG.

TABLE 1: Total (E_{total}) and Relative ($E_{relative}$) Energies of Various Possible $[GGGG + H - H_2O]^+$ Ions Determined at the B3LYP/6-31+G(d,p) Level of Theory with the Relative Energies Corrected for Zero-Point Vibration Energy (ZPE) at the B3LYP/6-31G(d) Level

	E_{total}/Hartrees	E_{total} + ZPE/Hartrees	$E_{relative}$/kcal mol^{-1}
I	−832.444155	−832.210377	0.0
II	−832.443991	−832.207471	1.8
III	−832.420212	−832.187007	14.7
IV	−832.420895	−832.184561	16.2
V	−832.423362	−832.190292	12.6
VI	−832.421344	−832.189352	13.2
VII	−832.422606	−832.186600	14.9
VIII	−832.420220	−832.186596	14.9

IRMPD Investigation of $[GGGG + H - H_2O]^+$. IRMPD spectroscopy was used to characterize the structure of the $[GGGG + H - H_2O]^+$ ion generated from protonated GGGG by comparison with the theoretical spectra generated from the DFT calculated structures, focusing on the conventional b_4 ion structures (Figure 1), which feature an oxazolone ring at the C-terminus and the oxazole-type ring structures (Figure 2), which feature an unaltered carboxylic acid C-terminus.

The principal difference in the oxazolone product ion structures is the site of protonation, located at either the oxazolone ring nitrogen or the N-terminus (structures **I** and **II** respectively, Figure 1, Table 1). Naturally, the site of protonation in each case directs the peptide backbone dihedral angles to enable stabilizing, intramolecular hydrogen bonding. Alternative protonation sites are theoretically possible but have previously been shown by theory and experiment not to be competitive.[3] The structures of the type proposed be Reid et al.[6b] (structures **III**−**VIII**, Figure 2, Table 1) are more than 10 kcal mol^{-1} less energetically favorable than the oxazolone forms of the $[GGGG + H - H_2O]^+$ ion, though it is important to note that generation of a particular product ion will be dependent on the relative activation energies and the associated kinetics of the two reaction pathways. The lowest energy nonoxazolone product, structure **VI**, features a protonated five-membered ring in the middle of the peptide backbone. Structures **VII** and **VIII** are of the same type but feature protonation at the N-terminus and imine nitrogen, respectively. The three other isomers of this product type (**III**−**V**) all feature the five-membered ring closer to the N-terminus of the product ion. These differ in the site of protonation; i.e., structure **III** is protonated on the N atom of

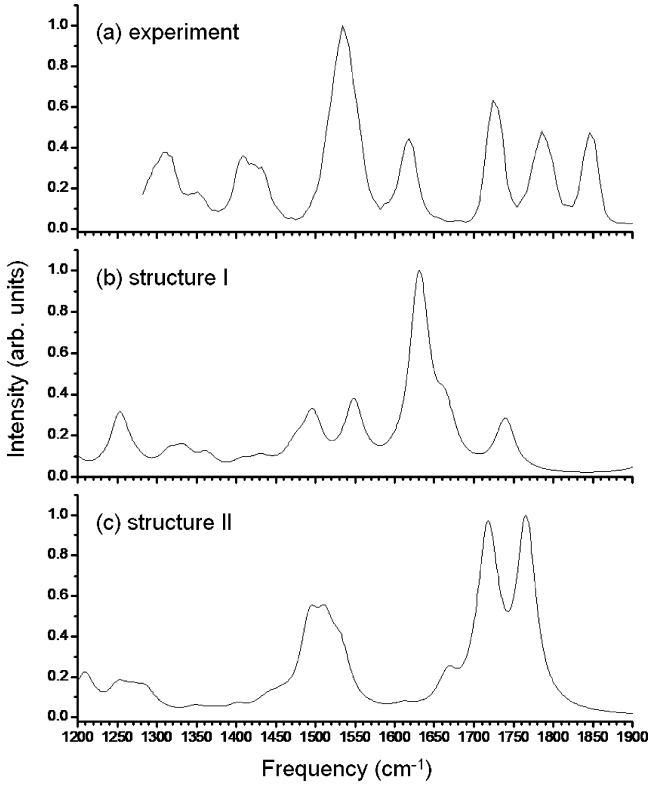

Figure 5. Comparison of IRMPD of $[GGGG + H - H_2O]^+$ derived from protonated GGGG to theoretical spectra of oxazolone b_4 structures: (a) experimental IRMPD spectrum; (b) theoretical spectrum of **I**, oxazolone nitrogen protonated; (c) theoretical spectrum of **II**, oxazolone N-terminally protonated.

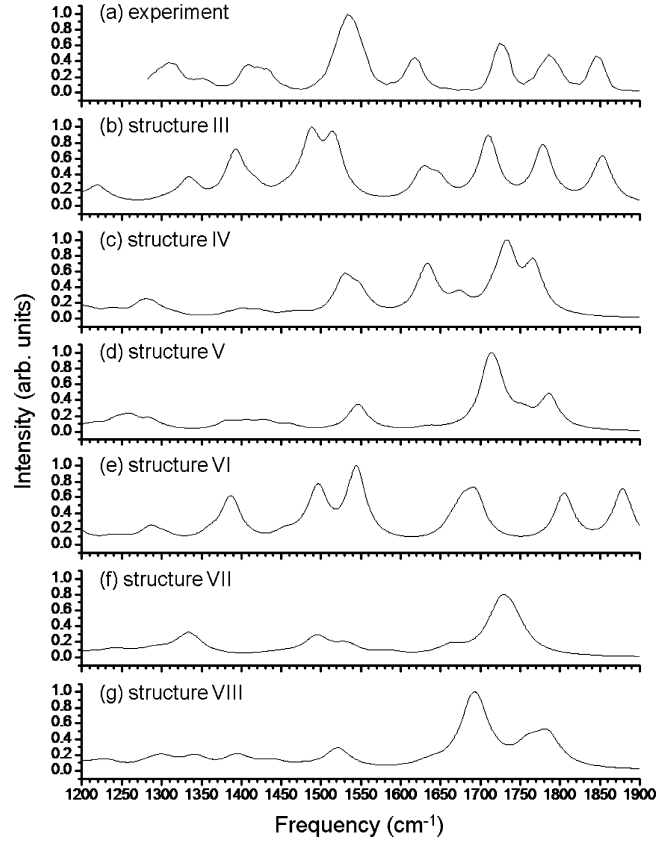

Figure 6. Comparison of IRMPD of $[GGGG + H - H_2O]^+$ derived from protonated GGGG to theoretical spectra of nonoxazolone structures: (a) experimental IRMPD spectrum; (b) theoretical spectrum of **III**, H_2O loss ring protonated; (c) theoretical spectrum of **IV**, H_2O loss N-terminally protonated; (d) theoretical spectrum of **V**, H_2O loss imine protonated; (e) theoretical spectrum of **VI**, protonated five-membered ring in the middle of the peptide backbone; (f) theoretical spectrum of **VII**, N-terminally protonated structure, with five-membered ring in the middle of the peptide backbone; (g) theoretical spectrum of **VIII**, imine protonated structure, with five-membered ring in the middle of the peptide backbone.

the five-membered ring, structure **IV** is protonated at the N-terminal amino group, while structure **V** is protonated at the N atom of the imine adjoining the five-membered ring in the backbone.

The experimental IRMPD spectrum (1200−1850 cm^{-1}) generated from $[GGGG + H - H_2O]^+$ produced from protonated GGGG is shown in Figure 5a. The theoretical spectra of the two oxazolone structures **I** and **II** are provided for comparison (Figure 5b,c, respectively). Neither of the theoretical b_4 oxazolone spectra matches the experimental IRMPD spectrum in terms of the positions or relative intensities of absorptions. This supports the preceding argument based on the MS^n data that the $[GGGG + H - H_2O]^+$ peak is primarily a nonoxazolone structure.

Figure 6 compares the theoretical spectra of structures **III**−**VII** to the experimentally recorded spectrum. The closest agreement between experiment and theory is provided by structure **III**, which features an intact C-terminal carboxyl group, a substituted oxazole ring close to the N-terminus and a nonprotonated imine group (Figure 2). Only the theoretical spectrum of this structure reproduces the three prominent absorptions between 1700 and 1900 cm^{-1} in the experimental IRMPD spectrum. On the basis of this assignment the absorptions in the experimental IRMPD spectrum located at ∼1730 and 1790 cm^{-1} correspond to the amide and carboxylic acid C═O stretches, respectively, while the absorption at ∼1850 cm^{-1} is the C═N stretch of the nonprotonated imine group. This imine stretch involves the C atom of the five-membered ring at the amino terminus and the N atom of the adjacent G residue. The remaining absorptions are also explained by this structure. The absorption at ∼1540 cm^{-1} appears to be composed of two unresolved N−H wag components (the first of the sole, intact amide group and the second of the N−H group of the five-membered ring at the amino terminus). The smaller absorption at ∼1620 cm^{-1} is assigned to a C═N stretch of the five-membered ring coupled to an N−H scissor mode of the free amino group at the N-terminus. The remaining absorptions below 1450 cm^{-1} in the IRMPD spectrum are assigned as backbone stretching modes that are less diagnostic of structure.

It should be noted that additional large ring type structures were also considered as candidates but resulted in extremely high energies, or collapsed to form one of the aforementioned structures in the manuscript. Additionally, despite the MS^n evidence, the structures of six-membered N-terminal ring structures that show some similarities to diketopiperazines were calculated to absolutely rule out this possibility. These structures (structures XI and XII) and spectra are shown in the Supporting Information in Figures S4 and S5, respectively. Comparison of experimental IRMPD spectra to those for structures XI and XII offer further support to our structural proposals based on tandem mass spectrometry, theoretical calculations and IRMPD action spectroscopy.

IRMPD Investigation of $[GGGG + H - H_2O - 29]^+$. The combined MS^n and IRMPD spectra indicate that structure **III** is the likely structure of the $[GGGG - H_2O + H]^+$ ions. The predominant peak resulting from MS^3 fragmentation of this ion is the $[GGGG - H_2O - 29 + H]^+$ peak. The two conceivable

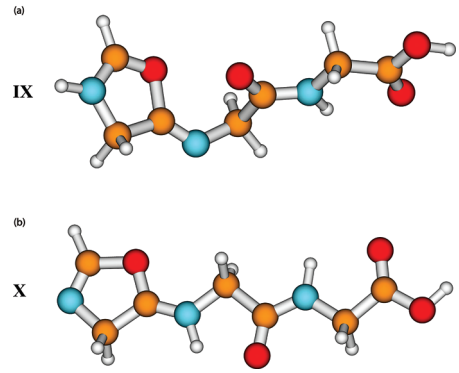

Figure 7. Possible structures of $[GGGG - H_2O - 29 + H]^+$ ions determined at the B3LYP/6-31+G(d,p) level of theory with the relative energies corrected for zero-point vibration energy (ZPE) at the B3LYP/6-31G(d): (a) **IX**, ring protonated; (b) **X**, imine protonated.

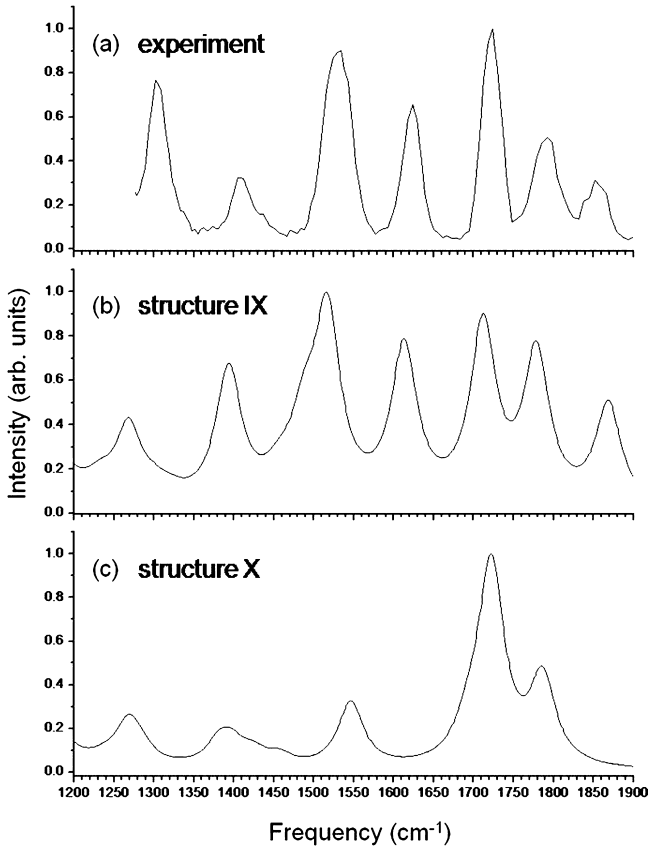

Figure 8. Comparison of IRMPD of $[GGGG - H_2O - 29 + H]^+$ derived from protonated GGGG to theoretical spectra of structures **IX** and **X**: (a) experimental IRMPD spectrum; (b) theoretical spectrum of **IX**, ring protonated; (c) theoretical spectrum of **X**, imine protonated. The theoretical spectra are plotted with a 40 cm^{-1} fwhm.

protonated forms of this ion are shown in Figure 7 and the experimental IRMPD spectrum of this ion together with the theoretical spectra for comparison are shown in Figure 8. The theoretical spectrum of structure **IX** is very similar to the experimental spectrum whereas that of structure **X** is not, despite being >10 kcal mol^{-1} more energetically favorable (Table S1, Supporting Information). This is due to the combined rigid ring and imine structure preventing proton transfers to the more energetically favorable imine protonation site.

Mechanism of $[GGGG - H_2O - 29]^+$ Ion Formation. Further support for our proposed structure is provided by TS calculations which show a transition structure requiring 32.2 kcal mol^{-1} (relative to structure **III,** Scheme 2, Table S2, Supporting Information) and no proton mobilization being necessary to generate the product ion assigned in the preceding IRMPD spectrum (Figure 8). This is logical as proton mobilization from the ring nitrogen in the rigid structure **III** would be extremely energetically demanding, unlike the observed primary fragmentation pathway calculated here. Similar mechanisms and observations have been proposed and made by El Aribi et al.[25]

SCHEME 2: Mechanism of $[GGGG + H - H_2O - 29]^+$ Formation Determined at the B3LYP/6-31+G(d,p) Level of Theory with the Relative Energies Corrected for Zero-Point Vibration Energy (ZPE) at the B3LYP/6-31G(d) Level

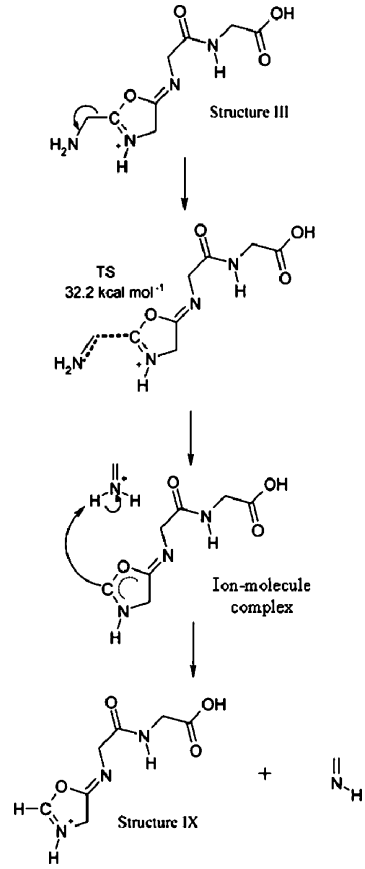

Conclusions

Multiple-stage tandem mass spectrometry, CID and wavelength-selective IRMPD were used to characterize the product ions generated by loss of H_2O from GGGX (X = G, A, and V) and GGGGG, and the losses of H_2O and CH_3OH from the methyl esters of these peptides. CID experiments show that $[M + H - H_2O]^+$ is the dominant peak generated from both GGGG and GGGG−OMe, thus suggesting that the species does not represent formation of b_4. Subsequent CID of $[M + H - H_2O]^+$ causes elimination of 29 mass units, which is inconsistent with the typical fragmentation behavior of protonated oxazolone b ions that would ordinarily be expected here. IRMPD spectroscopy and theoretical calculations of structure and IR frequencies confirm that $[GGGG + H - H_2O]^+$ is not an oxazolone but instead involves elimination of a non-C-terminal oxygen atom to produce a substituted oxazole ring near the amino terminus. This is in agreement with prior explanations[6b,16] concerning loss of water from some peptide ions. A mechanism is proposed on the basis of DFT calculations for fragmentation of this ion via expulsion of an N-terminal imine. Furthermore, this finding

highlights the importance of considering non-C-terminal or residue specific water loss as a potential source of peaks in MS/MS spectra and the potential implications this has for peptide sequencing.

Acknowledgment. Work by M.V.S., R.P.D., and S.S.C. was supported in part by a grant from the National Science Foundation (CAREER-0239800). Preliminary DFT calculations were performed at Wichita State University using resources of the High-performance Computing Center (HIPECC), a facility supported by the NSF under Grants EIA-0216178 and EPS-0236913 and matching support from the State of Kansas and HIPECC. Work by G.S.G. (under the INL LDRD Program) is supported by the U.S. Department of Energy, Idaho National Laboratory, DOE Idaho Operations Office Contract DE AC07 05ID14517. B.J.B. acknowledges the German Cancer Research Center (DKFZ), Heidelberg, for a guest scientist fellowship. B.P. thanks the Deutsche Forschungsgemeinschaft for a Heisenberg fellowship. J.O. and J.S. are supported by the Nederlandse Organisatie voor Wetenschappelijk Onderzoek (NWO). The excellent support by Dr. B. Redlich and others of the FELIX staff is gratefully acknowledged.

Supporting Information Available: MS and IRMPD spectra of the methylated forms of the GGGX peptides, ring structures, and tables of relative energies. This material is available free of charge via the Internet at http://pubs.acs.org.

References and Notes

(1) (a) Hunt, D. F.; Yates, J. R., III; Shabanonowitz, J.; Winston, S.; Hauer, C. R. *Proc. Natl. Acad. Sci.* **1986**, *83*, 6233. (b) Biemann, K. *Biomed. Environ. Mass Spectrom.* **1988**, *16*, 99. (c) Paizs, B.; Suhai, S. *Mass Spectrom. Rev.* **2005**, *24*, 508.

(2) (a) Tsang, C. W.; Harrison, A. G. *J. Am. Chem. Soc.* **1976**, *98*, 1301–1308. (b) Burlet, O.; Yang, C. Y.; Gaskell, S. J. *J. Am. Soc. Mass Spectrom.* **1992**, *3*, 337–344. (c) Tang, X.; Boyd, R. K. *Rapid Commun. Mass Spectrom.* **1992**, *6*, 651–657. (d) Tang, X.; Thibault, P.; Boyd, R. K. *Anal. Chem.* **1993**, *65*, 2824–2834. (e) Jones, J. L.; Dongré, A. R.; Somogyi, Á.; Wysocki, V. H. *J. Am. Chem. Soc.* **1994**, *116*, 8368–8369. (f) Cox, K. A.; Gaskell, S. J.; Morris, M.; Whiting, A. *J. Am. Soc. Mass Spectrom.* **1996**, *7*, 522–531. (g) Dongré, A. R.; Jones, J. L.; Somogyi, Á.; Wysocki, V. H. *J. Am. Chem. Soc.* **1996**, *118*, 8365–8374. (h) Harrison, A. G.; Yalcin, T. *Int. J. Mass Spectrom. Ion Processes* **1997**, *165*, 339–347. (i) Summerfield, S. G.; Whiting, A.; Gaskell, S. J. *Int. J. Mass Spectrom. Ion Processes* **1997**, *162*, 149–161. (j) Summerfield, S. G.; Cox, K. A.; Gaskell, S. J. *J. Am. Soc. Mass Spectrom.* **1997**, *8*, 25–31. (k) Tsaprailis, G.; Nair, H.; Somogyi, Á.; Wysocki, V. H.; Zhong, W.; Futrell, J. H.; Summerfield, S. G.; Gaskell, S. J. *J. Am. Chem. Soc.* **1999**, *121*, 5142–5154. (l) Csonka, I. P.; Paizs, B.; Lendavy, G.; Suhai, S. *Rapid Commun. Mass Spectrom.* **2000**, *14*, 417–427. (m) Wysocki, V. H.; Tsaprailis, G.; Smith, L. L.; Breci, L. A. *J. Mass Spectrom.* **2000**, *35*, 1399–1406. (n) Paizs, B.; Csonka, I. P.; Lendvay, G.; Suhai, S. *Rapid Commun. Mass Spectrom.* **2001**, *15*, 637–647.

(3) Polfer, N. C.; Oomens, J.; Suhai, S.; Paizs, B. *J. Am. Chem. Soc.* **2007**, *129*, 5887.

(4) Jorgensen, T. J. D.; Gardsvoll, H.; Ploug, M.; Roepstorff, P. *J. Am. Chem. Soc.* **2005**, *127*, 2785.

(5) Paizs, B.; Lendvay, G.; Vékey, K.; Suhai, S. *Rapid Commun. Mass Spectrum.* **1999**, *13*, 525–533.

(6) (a) Polce, M. J.; Ren, D.; Wesdemiotis, C. *J. Mass Spectrom.* **2000**, *35*, 1391. (b) Reid, G. E.; Simpson, R. J.; O'Hair, R. A. J. *Int. J. Mass Spectrom.* **1999**, *190*−*191*, 209. (c) Cordero, M. M.; Houser, J. J.; Wesdemiotis, C. *Anal. Chem.* **1993**, *65*, 1594.

(7) (a) Yalcin, T.; Khouw, C.; Csizmadia, I. G.; Peterson, M. R.; Harrison, A. G. *J. Am. Soc. Mass Spectrom.* **1995**, *6*, 1165. (b) Yalcin, T.; Csizmadia, I. G.; Peterson, M. B.; Harrison, A. G. *J. Am. Soc. Mass Spectrom.* **1996**, *7*, 233. (c) Harrison, A. G. *Mass Spectrom. Rev.* **2009**, *28*, 640.

(8) (a) Nold, M. J.; Wesdemiotis, C.; Yalcin, T.; Harrison, A. G. *Int. J. Mass Spectrom. Ion Processes* **1997**, *164*, 137. (b) Polce, M. J.; Ren, D.; Wesdemiotis, C. *J. Mass Spectrom.* **2000**, *35*, 1391. (c) Farrugia, J. M.; O'Hair, R. A. J.; Reid, G. E. *Int. J. Mass Spectrom.,* **2001**, *210*−*211*, 71. (d) Rodriquez, C. F.; Cunje, A.; Shoeib, T.; Chu, I. K.; Hopkinson, A. C.; Siu, K. W. M. *J. Am. Chem. Soc.* **2001**, *123*, 3006.

(9) (a) Polfer, N. C.; Oomens, J.; Suhai, S.; Paizs, B. *J. Am. Chem. Soc.* **2005**, *127*, 17154. (b) Bythell, B. J.; Erlekam, U.; Paizs, B.; Maître, P. J. *ChemPhysChem* **2009**, *10*, 883. (c) Yoon, S. H.; Chamot-Rooke, J.; Perkins, B. R.; Hilderbrand, A. E.; Poutsma, J. C.; Wysocki, V. H. *J. Am. Chem. Soc.* **2008**, *130*, 17644. (d) Oomens, J.; Young, S.; Molesworth, S.; van Stipdonk, M. *J. Am. Soc. Mass Spectrom.* **2009**, *20*, 334.

(10) (a) Bythell, B.; Somogyi, A.; Paizs, B. *J. Am. Soc. Mass Spectrom.* **2009**, *20*, 618. (b) Somogyi, A. *J. Am. Soc. Mass Spectrom.* **2008**, *19*, 1771.

(11) Chen, X.; Turecek, F. *J. Am. Soc. Mass Spectrom.* **2005**, *16*, 1941.

(12) (a) Paizs, B.; Lendvay, G.; Vékey, K.; Suhai, S. *Rapid Commun. Mass Spectrom.* **1999**, *13*, 525. (b) Paizs, B.; Suhai, S. *Rapid Commun. Mass Spectrom.* **2002**, *16*, 375. (c) Paizs, B.; Suhai, S. *J. Am. Soc. Mass Spectrom.* **2004**, *15*, 103. (d) Bythell, B. J.; Barofsky, D. F.; Pingitore, F.; Polce, M. J.; Wang, P.; Wesdemiotis, C.; Paizs, B. *J. Am. Soc. Mass Spectrom.* **2007**, *18*, 1291.

(13) Perkins, B. R.; Chamot-Rooke, J.; Yoon, S. H.; Gucinski, A. C.; Somogyi, A.; Wysocki, V. H. ; *J. Am. Chem. Soc.*, DOI: 10.1021/ja9054542.

(14) (a) Harrison, A. G.; Young, A. B.; Bleiholder, B.; Suhai, S.; Paizs, B. *J. Am. Chem. Soc.* **2006**, *128*, 10364. (b) Riba-Garcia, I.; Giles, K.; Bateman, R. H.; Gaskell, S. J. *J. Am. Soc. Mass Spectrom.* **2008**, *19*, 609. (c) Bleiholder, C.; Osburn, S.; Williams, T. D.; Suhai, S.; Van Stipdonk, M.; Harrison, A. G.; Paizs, B. *J. Am. Chem. Soc.* **2008**, *130*, 17774. (d) Harrison, A. *J. Am. Soc. Mass Spectrom.* **2008**, *19*, 1776. (e) Erlekam, U.; Bythell, B. J.; Scuderi, D.; Van Stipdonk, M.; Paizs, B.; Maître, P. 2009, *131* (32),11503−11508. (f) Fattahi, A.; Zekavat, B.; Solouki, T. *J. Am. Soc. Mass Spectrom.*, doi: 10.1016/j.jasms.2009.10.017.

(15) (a) Paizs, B.; Lendvay, G.; Vékey, K.; Suhai, S. *Rapid Commun. Mass Spectrom.* **1999**, *13*, 525. (b) Paizs, B.; Suhai, S. *Rapid Commun. Mass Spectrom.* **2002**, *16*, 375. (c) Paizs, B.; Suhai, S. *J. Am. Soc. Mass Spectrom.* **2004**, *15*, 103.

(16) Ballard, K. D.; Gaskell, S. J. *J. Am. Soc. Mass Spectrom.* **1993**, *4*, 477–481.

(17) O'Hair, R. A. J.; Styles, M. L.; Reid, G. E. *J. Am. Soc. Mass Spectrom.* **1998**, *9*, 1275.

(18) (a) Oepts, D.; van der Meer, A. F. G.; van Amersfoort, P. W. *Infrared Phys. Technol.* **1995**, *36*, 297. (b) Polfer, N. C.; Oomens, J. *Phys. Chem. Chem. Phys.* **2007**, *9*, 3804–3817.

(19) Valle, J. J.; Eyler, J. R.; Oomens, J.; Moore, D. T.; van der Meer, A. F. G.; von Helden, G.; Meijer, G.; Hendrickson, C. L.; Marshall, A. G.; Blakney, G. T. *Rev. Sci. Instrum.* **2005**, *76*, 023103.

(20) Mize, T. H.; Taban, I.; Duursma, M.; Seynen, M.; Konijnenburg, M.; Vijftigschild, A.; Doornik, C. V.; Rooij, G. V.; Heeren, R. M. A. *Int. J. Mass Spectrom.* **2004**, *235*, 243–253.

(21) (a) Wyttenbach, T.; Paizs, B.; Barran, P.; Breci, L.; Liu, D.; Suhai, S.; Wysocki, V. H.; Bowers, M. T. *J. Am. Chem. Soc.* **2003**, *125*, 13768. (b) Paizs, B.; Suhai, S.; Hargittai, B.; Hruby, V. J.; Somogyi, A. *Int. J. Mass Spectrom.* **2002**, *219*, 203.

(22) Case, D. A.; Pearlman, D. A.; Caldwell, J. W.; Cheatham, T. E., III; Ross, W. S.; Simmerling, C. L.; Darden, T. A.; Merz, K. M.; Stanton, R. V.; Cheng, A. L.; Vincent, J. J.; Crowley, M.; Tsui, V.; Radmer, R. J.; Duan, Y.; Pitera, J.; Massova, I. G.; Seibel, G. L.; Singh, U. C.; Weiner, P. K.; Kollmann, P. A. In AMBER 99; University of California: San Francisco, 1999.

(23) Frisch, M. J.; Trucks, G. W.; Schlegel, H. B.; Scuseria, G. E.; Robb, M. A.; Cheeseman, J. R.; Montgomery, J. R., Jr.; Vreven, T.; Kudin, K. N.; Burant, J. C.; Millam, J. M.; Iyengar, S. S.; Tomasi, J.; Barone, V.; Mennucci, B.; Cossi, M.; Scalmani, G.; Rega, N.; Petersson, G. A.; Nakatsuji, H.; Hada, M.; Ehara, M.; Toyota, K.; Fukuda, R.; Hasegawa, J.; Ishida, M.; Nakajima, T.; Honda, Y.; Kitao, O.; Nakai, H.; Klene, M.; Li, X.; Knox, J. E.; Hratchian, H. B.; Cross, J. B.; Bakken, V.; Adamo, C.; Jaramillo, J.; Gomperts, R.; Stratmann, R. E.; Yazyev, O.; Austin, A. J.; Cammi, R.; Pomelli, C.; Ochterski, J. W.; Ayala, P. Y.; Morokuma, K.; Voth, G. A.; Salvador, P.; Dannenberg, J. J.; Zakrzewski, V. G.; Dapprich, S.; Daniels, A. D.; Strain, A. C.; Farkas, O.; Malick, D. K.; Rabuck, A. D.; Raghavachari, K.; Foresman, K. B.; Ortiz, J. V.; Cui, Q.; Baboul, A. G.; Clifford, S.; Cioslowski, J.; Stefanov, B. B.; Liu, G.; Liashenko, P.; Piskorz, P.; Komaromi, I.; Martin, R. L.; Fox, D. J.; Keith, T.; Al-Laham, M. A.; Peng, C. Y.; Nanayakkara, A.; Challacombe, M.; Gill, P. M. W.; Johnson, B.; Chen, W.; Wong, M. W.; Gonzalez, C.; Pople, J. A. *Gaussian 03*, Revision D.01; Gaussian, Inc.: Wallingford CT, 2004.

(24) Molesworth, S.; Leavitt, C. M.; Groenewold, G. S.; Oomens, J.; Steill, J. D.; van Stipdonk, M. *J. Am. Soc. Mass Spectrom.*, doi: 10.1016/j.jasms.2009.06.007.

(25) El Aribi, H.; Orlova, G.; Rodriquez, C. F.; Almeida, D. R. P.; Hopkinson, A. C.; Siu, K. W. M. *J. Phys. Chem. B* **2004**, *108*, 18743–18749.

JP9113046